TiO2 MOCVD coating for photocatalytic degradation of ciprofloxacin using 365 nm UV LEDs - kinetics and mechanisms

Thibaut Triquet, Claire Tendero, Laure Latapie, Marie-Hélène Manero, Romain Richard, Caroline Andriantsiferana

TiO_2 MOCVD coating for photocatalytic degradation of ciprofloxacin using 365 nm UV LEDs - kinetics and mechanisms

Thibaut Triquet [a], Claire Tendero [b], Laure Latapie [a], Marie-Hélène Manero [a], Romain Richard [a], Caroline Andriantsiferana [a,*]

[a] Laboratoire de Génie Chimique, Université de Toulouse, CNRS, INPT, UPS, Toulouse, France
[b] Centre Inter-universitaire de Recherche et d'Ingénierie des Matériaux, Université de Toulouse, CNRS, Toulouse, France

A B S T R A C T

This work presents a solution for the photocatalytic degradation of the antibiotic ciprofloxacin (CIP) in water, without using P25 TiO_2 powder and thus getting rid of expensive separation steps. It consists in using a TiO_2 coating that is directly deposited on the optical window of a photocatalytic micro-reactor and 365 nm UV LEDs as radiation source. P25 TiO_2 powder was also studied as reference. HPLC-MS was used to determine the transformation products and the pathways reactions. CIP was slowly degraded by the photolysis reaction at 365 nm: (75 % removal after 8 h of UV irradiation). However, no significant decrease of the total organic carbon (TOC) was noticed, thus showing the presence of transformation products not degraded by the action of UV-light alone. For a low catalyst amount (*i.e* 0.12 g of TiO_2, whatever the form, powder or coating, per liter of contaminated water,), excellent CIP degradation by photocatalysis was observed. Complete CIP degradation after 1 h of irradiation was required using P25 and 8 h using TiO_2 coating. Different preferential reaction pathways were identified for both TiO_2 catalysts. The Langmuir-Hinshelwood model showed a very good representation of the kinetics, unlike its simplified pseudo-first order model. Photocatalysis experiments did not show a complete mineralization (60–70 % of TOC removal), but most of the aromatic transformation products were degraded. The last transformation products were identified as small aliphatic acids. There is therefore a real interest in using MOCVD coating of TiO_2 for sustainable wastewater treatment to avoid expensive catalyst separation. A study with a spiked real effluent from a wastewater treatment plant was performed and a satisfactory degradation was obtained. Slower kinetics were found due to the presence of additional organic products and scavenger compounds such as HCO_3^-.

1. Introduction

Although water is an important resource on earth, its purity is essential for human consumption. In the past decades, many toxic molecules such as micropollutants (i.e. pharmaceuticals products: antibiotics, anti-inflammatories, analgesics) are present in waterways and underground leading to serious consequences for the environment. Even if the concentration of these micropollutants are very low (ranging from $ng.L^{-1}$ to $\mu g.L^{-1}$), anthropogenic activity induces regular increase of their occurrence in natural waters. Due to this increase, global and European environmental standards have been lowered to reduce environmental concerns [1]. Among all micropollutants, the most persistent are fluoroquinolones such as ciprofloxacin (CIP). These molecules are of great danger for the ecosystems due to bioaccumulation, which leads to high toxicity levels [2]. Classical wastewater treatment (i.e. filtration, decantation, biological processes…) cannot totally eliminate these molecules and additional treatments are therefore required. Separation techniques such as adsorption and stripping processes can be used but also degradation techniques such as Advanced Oxidation Processes (AOP) (chemical oxidation/reduction) [3]. AOP degrade the target molecules [4,5] into inorganic compounds (production of water and carbon dioxide) or harmless transformation products [6]. AOP are furthermore very efficient due to the production of strong chemical oxidants, mainly hydroxyl radicals ($OH^{\bullet}$), which are strongly reactive due to their high oxidation potential [7–9]. Several AOP treatments have been studied and shown to be effective for the removal of fluoroquinolones. Individual processes (ozonation, photocatalysis, Fenton reaction…) and combined processes (O_3/UV, O_3/H_2O_2/UV and

* Corresponding author.
E-mail address: caroline.andriantsiferana@iut-tlse3.fr (C. Andriantsiferana).

https://doi.org/10.1016/j.jece.2020.104544

Table 1
Physico-chemical properties of CIP.

Molecule	Formula	Molar Weight (g. mol^{-1})	pK_a [39]	Solubility at 25 °C [40]
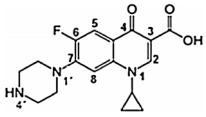	$C_{17}H_{18}FN_3O_3$	331.35	3.64 (N1); 5.05 (N1′); 6.95 (OH); 8.95 (N4′)	75 ± 10 $mg.L^{-1}$ in water 150 ± 5 $mg.L^{-1}$ in acetone 25 $g.L^{-1}$ in acidic water (pH = 3)

UV/H_2O_2) also provide interesting performances [10–12]. Amongst these AOP, photocatalysis is known to be an efficient technique to degrade organic compounds such as fluoroquinolones under both UV [13–15] and visible light [16–18]. This photochemical reaction occurs in presence of a metal oxide semiconductor catalyst. Titanium dioxide (TiO_2) is the most commonly used catalyst. Indeed, TiO_2 can absorb UV-light ($\lambda < 385$ nm) to create free electrons (e-) and free holes (h^+) [19]. TiO_2 is mostly used due to its low cost, photo-chemical stability. Furthermore, both its specific area and crystalline structures drive its photocatalytic efficiency [20]. The main drawback of using TiO_2 is the particle size: it is usually a powder composed of nanoparticles, which are suspected to increase the risk of chronic intestinal inflammation and carcinogenesis [21]. Due to the very small size of the catalyst, an expensive filtration step is therefore required after treatment in order to separate the catalyst from the water. To avoid this separation step, an alternative technique consists of using supported catalysts [22] on classical supports such as glass [23], metal [24], activated carbon [25, 26] or directly at the surface of a reactor [27]. To obtain a TiO_2 coating on the surface of a support, several techniques are available including sol-gel deposition [28], Metal Organic Chemical Vapor Deposition (MOCVD) [29], impregnation and oxidation processes [30] such as anodization technology [31] or plasma electrolytic oxidation [32]. MOCVD is of great interest since it allows the control of the physical characteristics of the coating, namely the crystalline structure and the morphology. Moreover, this deposition technique is known to ensure adherent and conformal coverage of high aspect ratio surfaces, regardless of the nature of the substrate (metal, glass or silicon). Therefore, this technique has been selected for this work along with glass as the support.

For this study, the selected fluoroquinolone target molecule is the antibiotic CIP, which is representative of a persistent micropollutant after conventional wastewater treatment [33,34]. To degrade this molecule, photocatalysis was investigated using a TiO_2 MOCVD coating on the upper glass window of a channel reactor and irradiated by a monochromatic LED lamp at 365 nm. The objective of this work is to study the performance of this catalyst under specific operating conditions where the quantity of catalyst used is 5–10 times lower than most of the work reported in the literature. The performance is then compared to the classical powder catalyst P25. In addition, a precise determination of the transformation products formed has been developed through the use of high-performance analytical techniques. Photocatalysis and photolysis experiments are compared with an objective of identifying the reaction pathways. This study also investigates the choice of an accurate model for the photocatalytic CIP degradation. The use of kinetics models can be an advantage for describing performances and to compare different catalysts. Two categories of models can be used: theoretical and empirical kinetics models [35]. In this study, theoretical kinetics model will be investigated. Most of the authors modelled the photocatalytic degradation with a first-order equation corresponding to a simplified Langmuir-Hinshelwood (L—H) model or with a second-order model [36]. However, these models are not always adequate due to simplifying assumptions which can be discussed [37]. Therefore, the L-H model, studied in this study, appears to be a more suitable and very effective modeling method [35]. Some authors also propose modelling by coupling mass-balance equations (considering time, convection and diffusion terms), reaction mechanisms of each species (reaction rate, adsorption coefficient and kinetics constants) [38]. Finally, the influence of the liquid matrix is investigated by replacing distilled water with a real effluent from a wastewater treatment plant.

Table 2
Analysis of the real effluent.

Analysis	Method	Results	Units
NH_4^+	ISO 11,732	<0.4	$mg_N.L^{-1}$
NO_3^-	ISO 13,395	<0.5	$mg_N.L^{-1}$
NO_2^-	ISO 13,395	<0.1	$mg_N.L^{-1}$
CO_3^{2-}	ISO 9963−1	<1	$m_{CO3}.L^{-1}$
HCO_3^-	ISO 9963−1	212	$mg_{HCO3}.L^{-1}$
Chemical Oxygen Demand (COD)	ISO 15,705	<0.5	$mg_{O2}.L^{-1}$
Biochemical Oxygen Demand (BOD)	1899−1	2.0	$mg_{O2}.L^{-1}$
Alkalimetric Title	ISO 9963−1	<5	ppm
Complete Alkalimetric Title	ISO 9963−1	174	ppm
pH	ISO 10,523	7.4 (at 19 °C)	–

Table 3
Operating conditions for MOCVD process.

Precursor temperature in the bubbler	50 °C
Deposition temperature	500 °C
Carrier gas (N_2) flow rate	25 $cm^3.min^{-1}$
Dilution gas (N_2) flow rate	500 $cm^3.min^{-1}$
Deposition pressure	5 Torr

2. Material and method

2.1. Chemicals

Analytical grade ciprofloxacin, $C_{17}H_{18}FN_3O_3$ (CIP, 98 % purity) with physico-chemical properties given in Table 1, TiO_2 powder (DEGUSSA-P25), formic acid, CH_2O_2 (formic acid, >99 % purity) and Titanium tetraisopropoxide (TTIP, 99.999 %) were purchased from Sigma Aldrich.

A water sample collected from the outlet of a wastewater treatment plant (Castanet-Tolosan, France) was analysed by the Departmental Laboratory 31: Water – Veterinary – Air in Launaguet (France). The following measurements were carried out: COD (Chemical Oxygen Demand), BOD (Biochemical Oxygen Demand), nitrite (NO_3^-), nitrate (NO_2^-), ammonium (NH_4^+), carbonates (CO_3^{2-}), bicarbonates (HCO_3^-), AT (Alkalimetric title) and CAT (Complete Alkalimetric title). The results are presented in Table 2.

2.2. MOCVD deposition

TiO_2 coating was grown in a tubular, horizontal hot-wall reactor that was described in [41], on Pyrex® glass and silicon substrates. Titanium tetraisopropoxide (TTIP, 99.999 %, Sigma-Aldrich) was thermally regulated in a bubbler and carried to the deposition zone, with 99.9992 % pure nitrogen as carrier gas. Table 3 summarizes the process conditions. Substrates were weighed before and after treatment to estimate the mass coated on the glass.

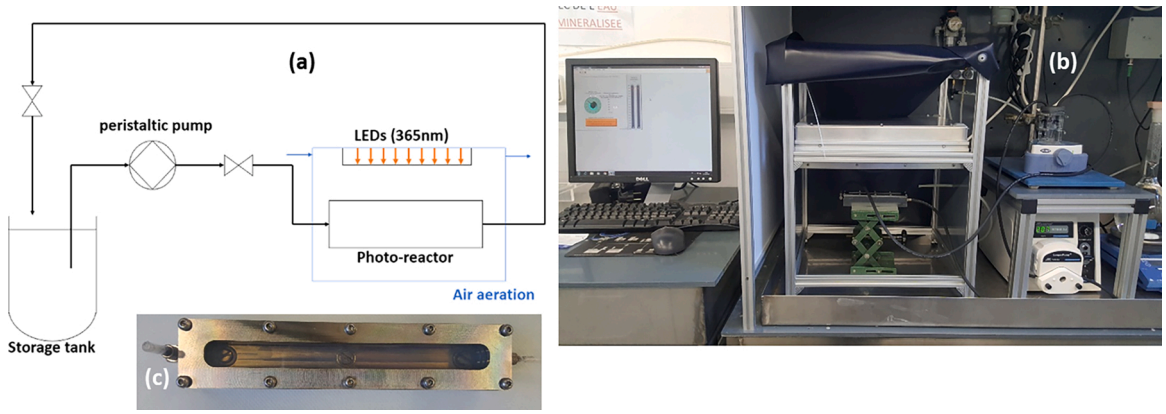

Fig. 1. Experimental setup representation (a); experimental setup (b); photo-reactor (c).

2.3. Characterization of the coating

Scanning Electron Microscopy (SEM, LEO-435 VP-PGT) was used to determine both the morphology and evaluate the thickness of the coating, which was deduced from cross-section measurements.

Atomic Force Microscopy (AFM, Agilent 5500) enabled the evaluation of the coating roughness.

The crystalline structure was deduced from X-Ray diffraction measurements under 2° grazing incidence with a Cu Kα anode in theta-theta mode (GI-XRD, Bruker D8).

UV–vis spectrometry (Perkin-Elmer LAMBDA 19) was finally used to characterize the optical properties of the samples such as transmittance and band-gap.

2.4. Experimental set-up

Fig. 1 represents the experimental set-up used for all photolysis and photocatalysis experiments. It consists of a 100 mL storage tank filled with the initial solution. A peristaltic pump at a constant flow rate (200 $mL.min^{-1}$) ensures the circulation between the tank and the photo-reactor equipped with a glass window (130 × 10 × 12 mm). A monochromatic LED panel (365 nm) is placed 15 cm above the reactor and irradiates the liquid inside the reactor. An air aeration system maintains the temperature at 25 °C (±1 °C).

2.5. Photolysis and photocatalysis experiments

Photolysis and photocatalysis reactions were carried out with the same experimental protocol. A first step of adsorption was performed for 1.5 h in the dark (UV off). An initial solution of 100 mL at 20 $mg.L^{-1}$ CIP was used. For each experiment, uniform irradiation was maintained for 8 h (Irradiance =10 $mW.cm^{-2}$, λ = 365 nm). For the photolysis experiments, the photo-reactor was equipped with a clean glass window, whereas for the photocatalysis experiments, a clean glass window with TiO_2 powder (12 ± 1 mg) or a glass window with the TiO_2 coating on its surface was used. The liquid samples were collected in the storage tank and filtered through a 0.45 µm Nylon membrane before being analyzed. Every experiment was carried out three times in order to determine the standard deviation.

The concentration of CIP used for this study was higher than classical concentrations measured inside water after wastewater treatment (20 $mg.L^{-1}$ vs C < 1 $\mu g.L^{-1}$). This choice was motivated by the operating conditions of the study (100 mL of treated solution). To analyze a solution with very low concentration, every sample has to be concentrated before the HPLC analysis. Therefore, the volume to be concentrated has to be between 500 mL and 1 L. In this study, a concentration step is then not possible due to the experimental device, which strongly limits the volume of the treated solution (only 100 mL). Under these conditions, the concentration of the initial solution has to be higher than the real effluent in order to analyze the solution and detect all transformation products formed. Moreover, the experimental device includes many elements (reactor, pump, tube, storage tank) and part of the CIP and transformation products could be absorbed inside the system, which would modify the results.

2.6. Analytical methods

To follow the concentration of ciprofloxacin during the process, each sample was analyzed by HPLC-UV. The HPLC used is a HPLC-PDA Thermo Accela (Shimadzu, Japan), equipped with a UV detector at 280 nm and a C18 column (2.6 µm, 100 mm x 3 mm). The method used for HPLC-UV is a multi-ramp. The mobile phase is fed by two channels two phases: (A) as acetonitrile and (B) as acidic water (0.1 % of formic acid). The mobile phase is firstly 90 % of B and 10 % of A. The percentage of A is then increased from 10 % to 90 % over 7 min and then held for 5 min. A ramp of 7 min is then used to return to 10 % of A and 90 % of B and this proportion is maintained for another 5 min. During the whole analysis, the flowrate was maintained at 0.3 $mL.min^{-1}$ at 40 °C.

For the determination of reactive intermediates, a HPLC-MS a Thermofisher UltiMate 3000 HPLC was used, coupled with an Orbitrap High Resolution Mass Spectrometer (HRMS - Exactive) equipped with an Electrospray ionisation source (ESI). The UV detector was set at 280 nm, a Gemini C18 column was used (3 µm, 100 mm × 2 mm). The flow rate was maintained at 0.2 $mL.min^{-1}$ at 40 °C. The mobile phase is similar to the classic HPLC-UV used for experiment (A/B). During the first 2 min of the run, the mobile phase was maintained at 10/90 (v/v), then a ramp was performed for 7 min to reach 90/10 (v/v). This composition was maintained for 8 min before another ramp to reach the initial composition of 10/90 (v/v). This composition was then maintained for 6 min until the next injection. For the determination of intermediates, positive and negative ionization modes of the MS were used.

TOC measurements were carried out with a TOC-L (Total Organic Carbon Analyzer) from Shimadzu (Japan). Each sample was firstly analysed to determine the organic carbon by a 20 µL injection then a second analysis of 50 µL with hydrochloric acid (0.1 $mol.L^{-1}$) was conducted to determine the inorganic carbon.

Lastly, reactive intermediates were analysed by Ionic Chromatography (IC) using a Thermo Scientific ICS 5000+ ion chromatography with a conductimetric detector. The anion column used is an AS19 (4 µm, 2 × 250 mm) with a flow rate of 0.250 $mL.min^{-1}$ at 25 °C. The mobile phase is a solution of KOH. For 10 min, a concentration of 5 $mmol.L^{-1}$ of KOH is maintained. A ramp is then set for 15 min to achieve a concentration of 45 $mmol.L^{-1}$ of KOH, which is maintained for 10 min. Finally, another ramp of 2 min enables the concentration to be decreased to 5 $mmol.L^{-1}$ of KOH.

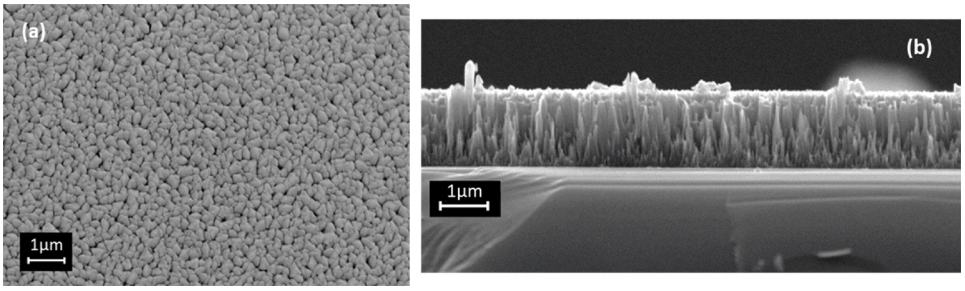

Fig. 2. SEM photos of TiO_2 coating on silicon substrate: (a) top view and (b) cross section of the coating.

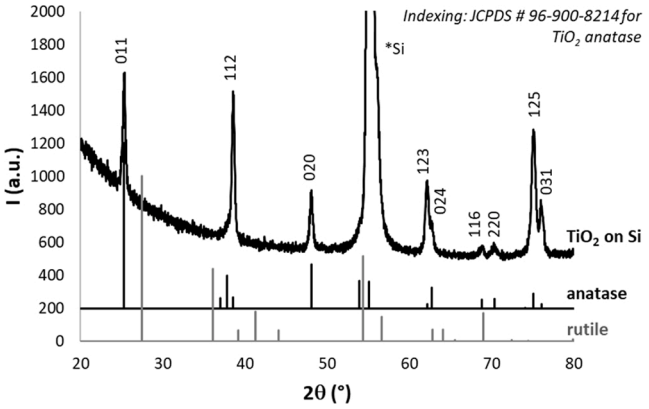

Fig. 3. XDR analysis of TiO_2 coating.

3. Results

3.1. Characterization of TiO_2 coatings

TiO_2 coatings were columnar as shown in the SEM photos given in Fig. 2. Fig. 2(a) shows a top view of the coating indicating full coverage of the substrate and Fig. 2(b) shows a cross section of the coating used to estimate its thickness at 1.6 ± 0.2 µm. The quadratic roughness (31 ± 1 nm) was deduced from AFM measurements.

The crystalline structure was a pure anatase, as confirmed by the XRD analysis: no peaks from the rutile structure were detected according to the JCPDS cards depicted for comparison as shown in Fig. 3. Previous work on TiO_2 structures [42] has shown that anatase phase has a better photocatalytic activity than other phases such as rutile or brookite.

UV–vis transmission measurements performed on the TiO_2 coated Pyrex at 200–800 nm highlight near total absorption of the UV LED radiation, as shown in Fig. 4. The interference fringes in the visible range were in agreement with the thickness of the coating estimated by SEM. Low transmittance can be seen at 365 nm, which is the wavelength used for the photocatalysis reaction. This coating will therefore have photocatalytic properties.

Moreover, in order to determine the optical band-gap Eg of the coatings, the Tauc plot [43] of the absorption coefficient α for indirect semi-conductors, deduced from transmission measurements as shown in Fig. 5 was used. A value of 3.1 eV is found, which is in agreement with a previous work for similar coatings [44].

3.2. Kinetics of photocatalysis

Fig. 6 shows a weak adsorption of CIP (3%) after 8 h in the glass and

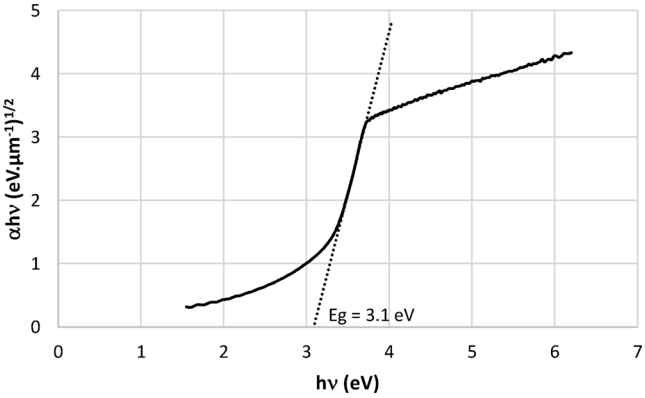

Fig. 5. Determination of the band gap energy of coating.

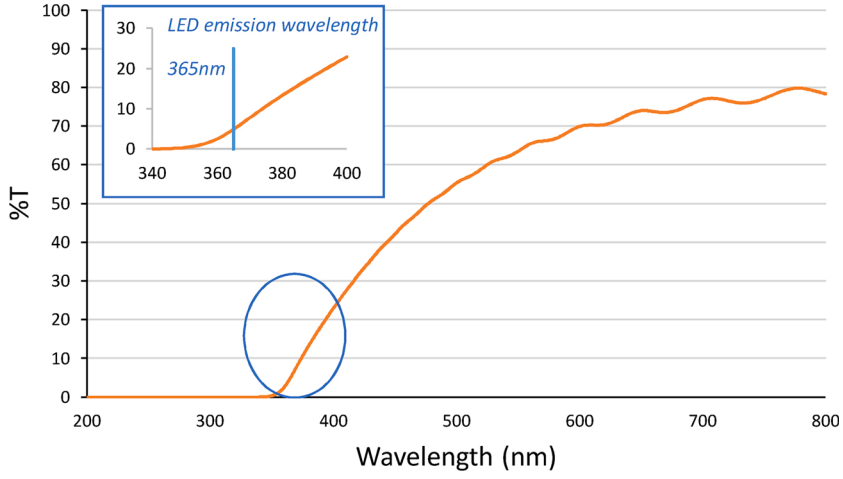

Fig. 4. UV–vis spectrum of coating.

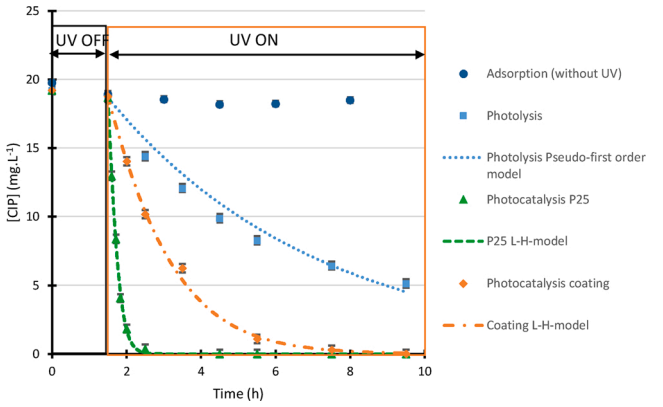

Fig. 6. Kinetics of degradation of ciprofloxacin by photolysis and photocatalysis.

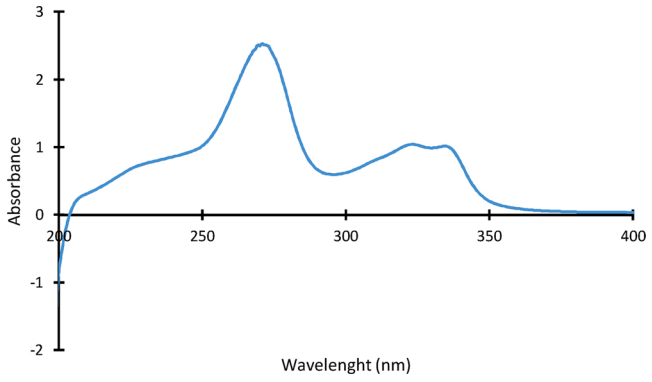

Fig. 7. Absorbance spectrum of ciprofloxacin.

hydraulic system, a significant degradation of CIP by photolysis (75 % after 8 h) and a total degradation of CIP by photocatalysis (with powder of TiO_2 – P25 and coating after respectively 1 h and 8 h).

Indeed, the photolysis of CIP was expected from its absorption UV-spectrum given in Fig. 7. The LED panel emitted UV at 365 nm and even though CIP absorbance is weak (0.071) for this wavelength, it appeared sufficient to eliminate ciprofloxacin by UV alone (photolysis reaction) [45].

In order to compare the TiO_2 powder and TiO_2 coating experiments, both experiments were carried out with a similar amount of TiO_2 (around 12 ± 1 mg). With the TiO_2 powder, less than 30 min of irradiation were required to remove 75 % of CIP, whereas 8 h were necessary with direct photolysis. Moreover, it was observed that CIP was totally degraded by photocatalysis with the P25 powder after 1 h of irradiation. Other studies have reported the same trend with TiO_2 powder: CIP could be degraded by both techniques with faster kinetics obtained with photocatalysis [45,46,14]. For photocatalysis with TiO_2 coating, 5 h of irradiation were necessary to eliminate 75 % of CIP and 8 h for a total degradation. This phenomenon has been already reported with methylene blue and carbamazepine [47,23]. It clearly appeared that a faster kinetic degradation of CIP was achieved with TiO_2 powder than with the coating. In the case of TiO_2 coating, even if the mass of the coating was equal to the amount of powder, part of the coating could not react with the liquid phase. This is due to the fact that the coating was fixed on the glass and therefore not directly available. Moreover, when the TiO_2 powder was used, the photocatalyst was homogeneously distributed in the liquid and directly in contact with CIP molecules which implied a faster reaction. The hydrodynamics inside the reactor was assessed, and the flow was laminar (Reynolds number of 303). In laminar flow, there is not enough turbulence to allow efficient contact between the liquid and the coating. To improve the kinetics, a higher flowrate should be used.

Table 4
Kinetics coefficients of CIP degradation.

	Pseudo-first order Simplified model ($K_{ad}C << 1$)		Langmuir-Hinshelwood model			
Study	k_{app} (min^{-1})	r^2	K_{ad} (L. mg^{-1})	k (mg. L^{-1}. min^{-1})	kK_{ad} (min^{-1})	$\sum(C_{mod}-C_{exp})^2$
P25	0.0648	0.986	0.0533	1.961	0.105	0.4146
Coating	0.0085	0.993	0.0284	0.343	0.0097	0.0018

However, this configuration has been chosen to have a longer irradiation time (i.e. long residence time for a small reactor). With a higher flowrate, the CIP would not have enough time to react inside the reactor since the residence time would be too short.

Experimental data were used to determine various kinetic parameters. First, the kinetic parameters of photolysis reaction were determined using a first-order kinetic model (1) [48,49]:

$$-\frac{dC}{dt} = k_{photolysis}C \quad (1)$$

A combination of the photolysis model with the complete Langmuir-Hinshelwood model was used to predict the degradation of the CIP during photocatalysis experiments:

$$-\frac{dC}{dt} = \frac{kK_{ad}C}{1+K_{ad}C} + k_{photolysis}C \quad (2)$$

where C represents the concentration of CIP, k is the kinetic constant of photocatalysis reaction, K_{ad} is the adsorption constant on the surface of catalyst and $k_{photolysis}$ is the kinetic constant of photolysis reaction.

In the literature [36], most authors have simplified the Langmuir-Hinshelwood model by considering the product $K_{ad}C << 1$. In this case, the model can be simplified and takes the form of a pseudo-first order kinetic model where $kK_{ad} = k_{app}$.

$$-\frac{dC}{dt} = kK_{ad}C + k_{photolysis}C = k_{app}C + k_{photolysis}C \quad (3)$$

Both photocatalysis models have been investigated due to new contradictory results [37], where the pseudo-first order seems not suitable for photocatalysis modelling. The aim of this modelling is to show which model can be used for this system.

A classical method of determining non-linear equations has been used for the Langmuir-Hinshelwood coefficients. This method was applied via a MatLab code using the simulannealbnd function [50,51] and using the minimisation of the summation of the square of the difference between calculated and experimental concentrations as convergence criteria.

Kinetic degradation by photolysis reaction was studied and the classic first order kinetic model gave good results. As shown in Fig. 6, this model represents rather correctly the CIP elimination ($r^2 = 0.959$) and the kinetic constant obtained $k_{photolysis}$ was estimated at 0.00295 min^{-1}.

For photocatalysis experiments, the Langmuir-Hinshelwood model (Eq. 2) was compared to a pseudo-first order model (Eq. 3). For both models, the value of $k_{photolysis}$ used was the value estimated previously. The parameters obtained with the TiO_2 coating and P25 TiO_2 for both models are presented in Table 4. The pseudo-first order kinetic model showed a good representation of the CIP degradation ($r^2 > 0.98$), however its use will be discussed. An excellent agreement was obtained between the Langmuir-Hinshelwood kinetic models and the experimental values as shown in Fig. 6. Value for pseudo-first order kinetic calculated in Table 4 for P25 is comparable to the literature value for photocatalysis of diclofenac with P25: 0.06 min^{-1} (which is also an antibiotic with similar formula as ciprofloxacin) [52].

An significant difference between values of k_{app} and the product kK_{ad} was noticed: 0.0648/0.105 min^{-1} for P25 and 0.0085/0.0097 min^{-1} for

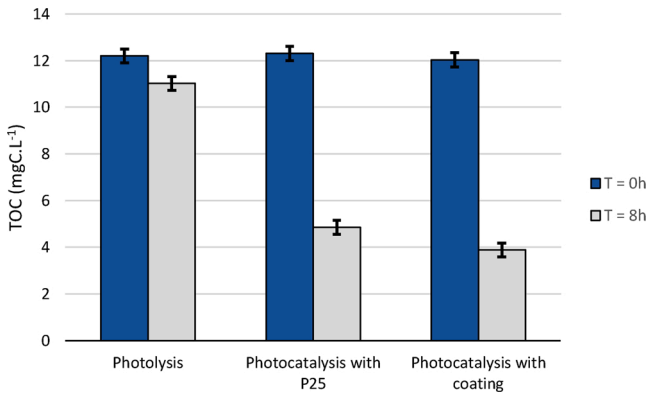

Fig. 8. Evolution of TOC in photolysis and photocatalysis reaction before and after treatment.

the TiO_2 coating. These deviations show that the hypothesis of $K_{ad}C <<< 1$ cannot be verified. Indeed, the values of $K_{ad}C$ are equal to 1.07 for P25 experiments and 0.57 for coating experiments respectively. The pseudo-first order model is not adapted to these kinetic representations: the Langmuir-Hinshelwood model cannot be simplified as systematically proposed in most publications.

To follow the mineralisation rate of the CIP in solution, a TOC (Total Organic Carbon) measurement was done before and after treatment (8 h). Fig. 8 represents the evolution of TOC for the different experiments. With the photolysis treatment of the solution, 75 % of CIP was degraded but the TOC was decreased by only 9.7 %. This means that photolysis completely degraded the CIP but not all the transformation products. Photolysis is a selective reaction; it can only degrade organic compounds which absorbed UV at the same wavelength as the lamp.

Concerning the photocatalysis experiments, a significant degradation of TOC was obtained: 61 % with P25 and 68 % with the coating. Due to the photocatalyst, CIP and an important part of the transformation products can be degraded. There was no significant difference between the powder and the coating. However, although there was a significant decrease of the TOC, there was no total mineralisation of the CIP. Other molecules were present in the solution and have to be identified.

3.3. *Transformation products*

Despite the fact that CIP was totally degraded by photocatalysis, some of the transformation products still remained in the solution. By following the production and degradation of these transformation products, it is possible to explain why the total mineralisation was not achieved. All aromatic transformation products were identified by HPLC-MS [14] and all of the suspected aromatic transformation products are listed in Table 5. These transformation products are representative of three different reaction pathways: oxidation/defluorination, dealkylation and oxidation. Through this analysis, it is possible to track their production and consumption during each experiment. Each retention time for HPLC analysis at 290 nm was assigned and the transformation products were followed by the evolution of the HPLC peak area. The evolution is shown in Fig. 9.

As shown in Fig. 9(a), during photolysis, ten different aromatic

Table 5
Transformation products: molecule structure, reaction pathway and HPLC retention time.

Molecule	Molecule structure [14]	Retention time (min)	Reaction pathway	Detection		
				Photolysis	Photocatalysis P25	Photocatalysis coating
A	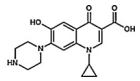	3.0	Oxidation Defluorination	Yes	Yes	Yes
B	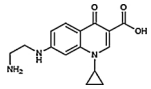	3.1	Oxidation Defluorination	Yes	Yes	Yes
C	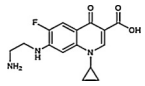	3.3	Dealkylation	Yes	Yes	Yes
D	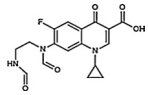	4.06	Oxidation	Yes	Yes	Yes
E	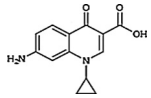	4.37	Dealkylation Defluorination	Yes	Yes	Yes
F	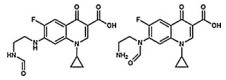	4.6	Oxidation	Yes	Yes	Yes
G	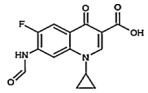	4.72	Oxidation	Yes	Yes	Yes
H	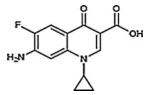	4.98	Dealkylation	Yes	Yes	Yes
I	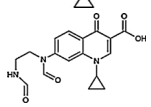	3.9	Oxidation Defluorination	Yes	Yes	No
J	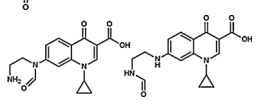	4.3	Oxidation Defluorination	Yes	No	No

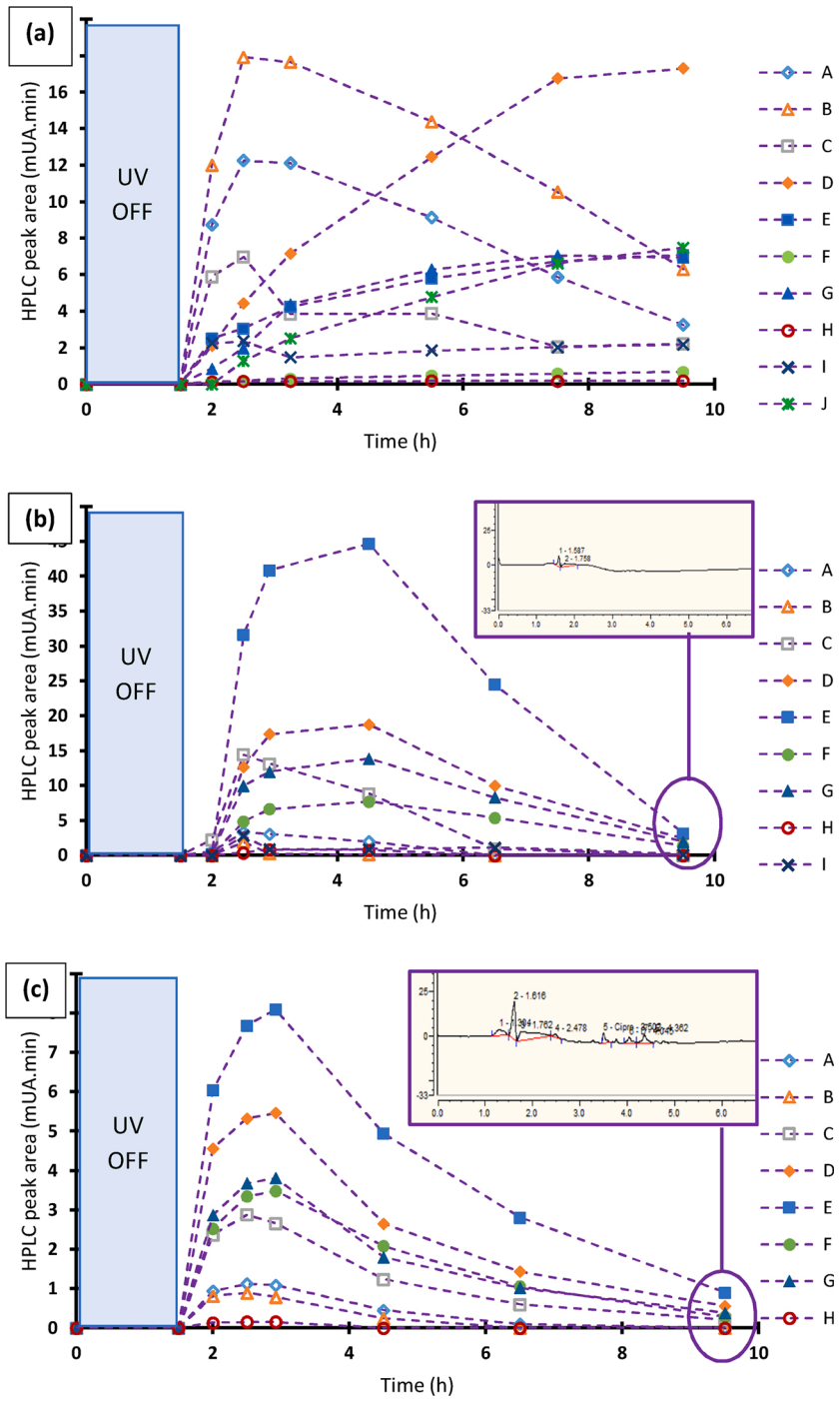

Fig. 9. Evolution of transformation products by photolysis (a), photocatalysis with P25 (b) and coating (c) reactions and last chromatogram for photocatalysis reaction.

transformation products were found. While these transformation products were quickly produced, their degradation was weak and slow. Some of them were not degraded; they showed stability to the degradation reaction under UV light (for 8 h of UV treatment). The slow TOC decrease can be explained by the non-degradation of these aromatic transformation products. Photolysis is a selective phenomenon as it can only degrade organic compounds that can absorb at the wavelength of the light used [53]. In this study a monochromatic light at 365 nm was used; the transformation products may not absorb this specific wavelength and hence were not degraded by photolysis. With this specific wavelength, only weak bonds (C–F) or non-aromatic cyclic compounds ($C_4N_2H_9$) seem to be broken.

In contrast, Fig. 9(b) and Fig. 9(c) show that all photocatalysis transformation products were formed and degraded during irradiation. While photolysis is a selective phenomenon, photocatalysis is a non-selective process. Through the production of super reactive radicals, many organic compounds can be degraded by the attack of these powerful oxidants. In this study, all transformation products were monitored by HPLC-UV at 290 nm, which is the representative wavelength of aromatic compounds. Nevertheless, at the end of the process, every aromatic compound was mostly degraded as shown in the last chromatogram in Fig. 9 regardless of the form of the catalyst (TiO_2 coating or P25). The main difference between using P25 and TiO_2 coating is the quantity of transformation product produced. A higher

Table 6
Identification and quantification of the final compounds present in water after treatment.

Ions	F^- ($mg.L^{-1}$)	$HCOO^-$ ($mg.L^{-1}$)	$C_2O_4^{2-}$ ($mg.L^{-1}$)
Pure water	–	0.02	–
Coating	0.960 ± 0.003	0.810 ± 0.006	0.360 ± 0.004
P25 TiO_2	1.060 ± 0.006	1.04 ± 0.02	0.210 ± 0.001
Photolysis	0.610 ± 0.003	0.620 ± 0.002	–

amount of transformation products was formed with P25 due to the fast degradation of CIP. For example, the maximum HPLC peak area for transformation product A was 44.7 mUA.min for P25 while it was only 8.1 mUA.min for TiO_2 coating. When TiO_2 coatings was used, fewer transformation products were created than with P25 or pure UV: 8 products with TiO_2 coating compared with 9 products with P25 TiO_2 and 10 products by photolysis. Two reaction pathways seem to be preferential with TiO_2 coating: the oxidation and dealkylation pathways. However, the kinetics of the oxidation and dealkylation reactions could be faster than defluorination kinetics.

For both photocatalytic experiments, the TOC values remained high (32 % for the coating and 39 % for P25) indicating that other organic compounds were present. Indeed, the presence of smaller organic compounds that were not degraded was expected. The last sample of each experiment was analysed by ionic chromatography. Table 6 shows the identification and quantification of compounds present at the end of treatment. At least three different aliphatic acids were found: formic acid, oxalic acid, as well as acetic and/or propionic acids, which have the same retention time. As expected from the oxidation, defluorination and dealkylation pathways, the other compounds detected were as follows: F^-, NO_2^-, NO_3^{2-}.

The last sample from each experiment presented a weak presence of small aliphatic acids: formic and oxalic acids. Under these experimental conditions (pH = 6.7 ± 0.1), formic acid was present in form of formate anion ($HCOO^-$) and oxalic acid in form of oxalate dianion ($C_2O_4^{2-}$). These two ions were present in low concentrations: 0.810 $mg.L^{-1}$ (formate) and 0.360 $mg.L^{-1}$ (oxalate) for the coating and 1.04 $mg.L^{-1}$ (formate) and 0.210 $mg.L^{-1}$ (oxalate) for the P25 TiO_2. From these concentrations, the carbon concentration from these ions could be determined which was found to represent 0.31 $mg_C.L^{-1}$and 0.33 $mg_C.L^{-1}$, which was only 8.1 % and 6.9 % of the final TOC for the coating and P25 TiO_2 respectively.

The CIP molecule has only one fluorine atom, therefore the maximum quantity of residual fluorine in the liquid phase has to be equal to the molar number of initial CIP (6.04×10^{-6} mol), which represents 1.15 $mg_F.L^{-1}$. The analysis of the last sample showed a lower concentration of fluorine than expected (0.96 $mg_F.L^{-1}$ for the coating and 1.06 $mg_F.L^{-1}$ for P25 TiO_2). Due to this difference, remaining fluorine atoms were still attached to carbon aromatic rings. As shown in Fig. 9(b) and (c), some aromatic transformation products could still be present in the water. Due to their large number of carbon atoms, even a small amount of them can have a significant impact on the value of the TOC explaining a non-zero TOC at the end of the treatment. It is therefore possible that a large part of the remaining TOC is due to the presence of these aromatics in small quantities. Even if the performances of photocatalysis are not entirely satisfactory at the high concentration of CIP tested (20 $mg.L^{-1}$), it is reasonable to expect that this photocalysis process to eliminate CIP may lead to better performances at environmental concentrations (< 1 $\mu g.L^{-1}$).

The use of TiO_2 coating is part of sustainable processes. A glass window with a TiO_2 coating can be used several times in a row. The same glass window was used to treat five different initial solutions of ciprofloxacin at 20 mg/L of 100 mL. For these reuses, the same kinetic and mineralization performances were obtained, which shows the suitability of this process.

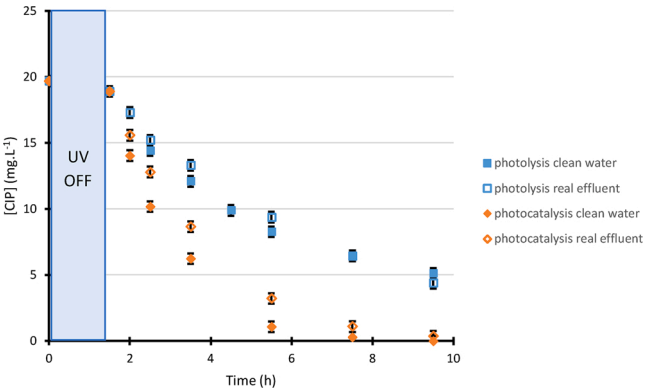

Fig. 10. Comparison of CIP degradation in ultra-pure water and a real effluent.

3.4. Analysis of a real effluent

The same experiments were carried out with a spiked real effluent for which the composition is given in Table 2. Fig. 10 compares the previous results obtained using ultra-pure water with the photolysis and photocatalysis (with coating) reaction performance using the real effluent. Only photocatalysis with coating was investigated because of the good efficiency obtained in clean water. With the real effluent, slower kinetic degradations were observed. For photolysis, 35 % of CIP still remains after 8 h of irradiation (compared with 20 % when using clean water) and for photocatalysis, 6 % of CIP remains after 8 h of irradiation (compared with less than 1 % when using clean water).

These differences could be explained by the complex nature of the real effluent which can strongly affect the performance of photocatalysis. A high TOC value of the real effluent was found (TOC = 40 $mg_C.L^{-1}$) in comparison with ultra-pure water (13 $mg_C.L^{-1}$). This higher value was due to the presence of organic compounds in this effluent and some of them are probably hardly oxidizable. That is why the organic compounds already present in the solution compete with CIP. The same interpretation explains the lower performance of photolysis with a TOC decrease of only 1 $mg_C.L^{-1}$ (TOC_f = 39 $mg_C.L^{-1}$).

Compounds such as inorganic ions were also present (HCO_3– for example), having a well-known scavenger effect. The same trend was observed during the photocatalytic degradation of carbamazepine [54] and cylindrospermopsin [55]. Indeed, HCO_3– ions can directly react with hydroxyl radicals in order to create other radicals ($CO_3^{2-\bullet}$) that are more highly selective and less reactive. Thus, reactive site of TiO_2 were less readily available for the degradation of CIP or transformation products. After photocatalytic degradation, 20 $mg_C.L^{-1}$ still remained in the solution corresponding to 50 % of TOC decrease.

As in ultra-pure water experiment, CIP was totally removed after 8 h (10 h in real effluent) but a total mineralisation was not reached even after 8 h of treatment. Fig. 11 shows the same trend for both reactions; many transformation products still remained in solution after 8 h of UV-treatment. The photocatalysis reaction results in better performance than photolysis although all aromatic transformation products were still detected in the solution. As for CIP, the degradation kinetics of the transformation products were slower in this complex matrix due to the presence of other organic compounds. Nevertheless, even if the degradation was incomplete after 8 h of irradiation, the concentration of these molecules decreased thereby showing the non-selectivity of photocatalysis. On the other hand, some transformation products did not seem to be degraded by photolysis showing its selectivity and confirming the efficiency of the photocatalytic process.

4. Conclusion

The TiO_2 coating presented interesting photocatalytic properties even with smaller amount of TiO_2 deposited compared to most studies.

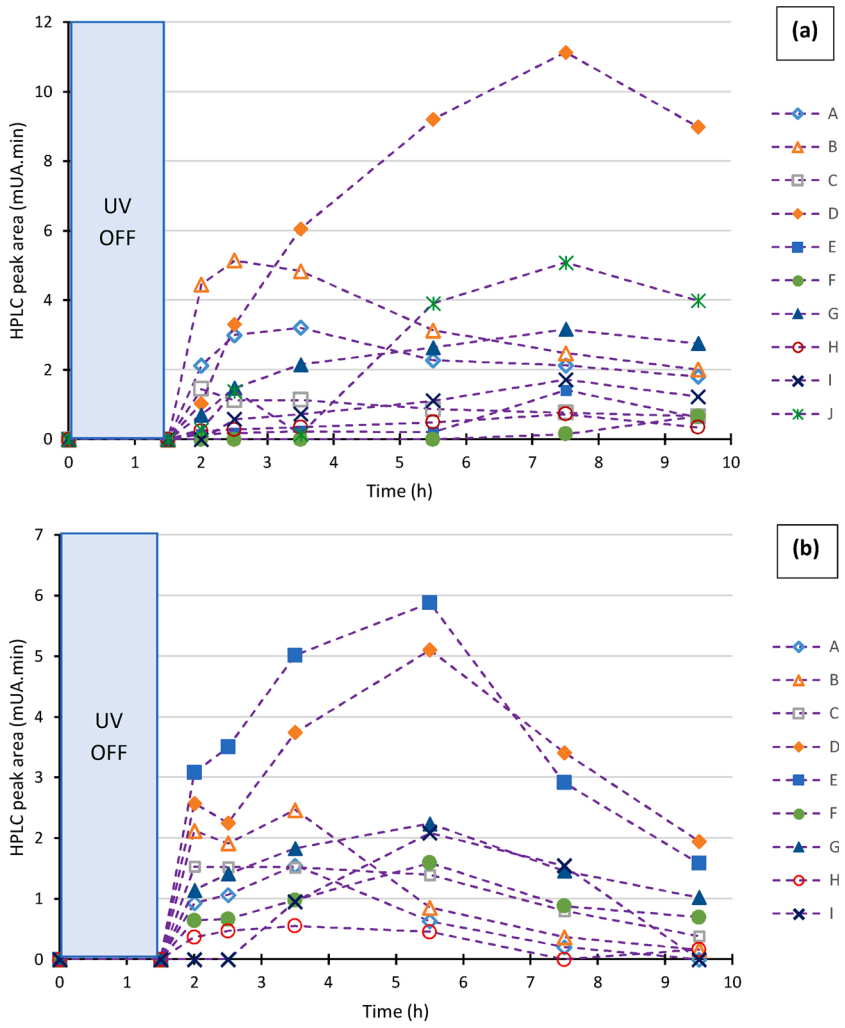

Fig. 11. Evolution of transformation products during (a) photolysis and (b) photocatalysis (coating) experiments with the spiked real effluent.

This study shows that antibiotics such as CIP can be degraded by a photocatalysis reaction using a wavelength present in solar radiation (365 nm) without doping the catalyst. Photocatalysis is confirmed as a non-selective process whereas photolysis is confirmed as a selective one. As expected, CIP can be degraded by photolysis, however most of the transformation products remain stable. The TiO_2 coating showed a slower degradation with CIP than with P25 but less transformation products were formed. The degradation by photocatalysis with both P25 and TiO_2 coating showed that most of the transformation products were degraded with 61 % and 68 % of TOC degradation respectively. The final transformation products were essentially aromatics molecules and small aliphatic acids (oxalic, formic, propionic and acetic acids). Concerning the chemical mechanisms, three different pathways, were identified – namely oxidation, alkylation and defluorination – by the presence of transformation products detected. Concerning the representation of kinetics degradation of CIP, the pseudo-first order model cannot be used even if the concentration of CIP is small ($K_{ad}C$ values close to 1), however excellent representation by the Langmuir-Hinshelwood has been noticed with a value of 0.0284 $L.mg^{-1}$ for K_{ad} and 0.343 $mg.L^{-1}.\ min^{-1}$ for k (for coating experiment). Moreover, the set-up used for photocatalysis experiments with TiO_2 coating proved its suitability: a same TiO_2/window glass can be used several times without being saturated. Experiments with a real effluent show satisfactory efficiency for the photocatalytic degradation of antibiotics using MOCVD coating, despite a high TOC value and the presence of scavengers such as inorganic ions.

Credit author statement

Caroline Andriantsiferana and Claire Tendero, conceived, supervised and designed the experiments. Thibaut TRIQUET performed the experiments, HPLC and TOC analysis and did the calculation for each kinetics models. Laure Latapie did every HPLC-MS analysis. Claire Tendero did the TiO_2 coating on glass by MOCVD with all characterizations of it (SEM, AFM, XRD). Thibaut TRIQUET, Claire Tendero, Caroline Andriantsiferana, Laure Latapie, Romain Richard and Marie-Hélène Manero wrote the paper.

Declaration of Competing Interest

The authors declare that they have no known competing financial interests or personal relationships that could have appeared to influence the work reported in this paper.

Acknowledgements

We would like to express kind regards to Pierre Albrand from Laboratoire de Génie Chimique (Université de Toulouse, CNRS, INPT, UPS, Toulouse, France) for his help to create the MATLAB code for kinetics coefficient determination. We would also like to express kind regards to the “Pole LCMS” from Laboratoire de Génie Chimique (Université de Toulouse, CNRS, INPT, UPS, Toulouse, France) for their help for the identification of transformation products by LCMS.

References

[1] MEEDDM, Recueil De Textes Sur l'assainissement, 2009.

[2] A. Moreira Meireles, A.L. Almeida Lage, A. Capelão Marciano, J. Martins Ribeiro, E.M. De Souza-Fagundes, D. Carvalho da Silva Martins, Ciprofloxacin degradation by first-, second-, and third-generation manganese porphyrins, J. Hazard. Mater. (2018) 445–451.

[3] K. Sivagami, K. Sakthivel, I.M. Nambi, Advanced oxidation processes for the treatment of tannery wastewater, J. Environ. Chem. Eng. 6 (2018) 3656–3663.

[4] K. González-Labrada, R. Richard, C. Andriantsiferana, H. Valdés, U.J. Jáuregui-Haza, M.-H. Manero, Enhancement of ciprofloxacin degradation in aqueous system by heterogeneous catalytic ozonation, Environ. Sci. Pollut. Res. - Int. 24 (2020) 1246–1255.

[5] T. Merle, J.-S. Pic, M.-H. Manero, S. Mathé, H. Debellefontaine, Influence of activated carbons on the kinetics and mechanisms of aromatic molecules ozonation, Catal. Today 151 (1–2) (2010) 166–172.

[6] R. Andreozzi, V. Caprio, A. Insola, R. Marotta, Advanced oxidation processes (AOP) for water purification and recovery, Catal. Today 53 (1999) 51–59.

[7] S. Abha, A. Javed, S.J.S. Flora, Application of advanced oxidation processes and toxicity assessment of transformation products, Environ. Res. 167 (2018) 223–233.

[8] S. Jiménez, M. Andreozzi, M.M. Micó, M.G. Álvarez, S. Contreras, Produced water treatment by advanced oxidation processes, Sci. Total Environ. 666 (2019) 12–21.

[9] W. Aboussaoud, M.-H. Manero, J.-S. Pic, H. Debellefontaine, Combined ozonation using alumino-silica materials for the removal of 2,4-Dimethylphenol from water, Ozone Sci. Eng. 36 (3) (2014) 221–228.

[10] T. Agustina, H. Ang, V. Vareek, A review of synergistic effect of photocatalysis nd ozaonation on wastewater treatment, J. Photochem. Photobiol. C Photochem. Rev. (2005) 264–273.

[11] K. González-Labrada, D.R. Alcorta Cuello, I. Saborit Sánchez, M. García Batle, M.-H. Manero, L. Barthe, U.J. Jáuregui-Haza, Optimization of ciprofloxacin degradation in wastewater by homogeneous sono-Fenton process at high frequency, J. Environ. Sci. Health 53 (2018) 1139–1148.

[12] P. Ajo, S. Preis, T. Vornamo, M. Mänttäri, M. Kallioinen, M. Louhi-Kultanen, Hospital wastewater treatment with pilot-scale pulsed corona discharge for removal of pharmaceutical residues, J. Environ. Chem. Eng. 6 (2018) 1569–1577.

[13] T. Paul, M.C. Dodd, T.J. Strathmann, Photolytic and photocatalytic decomposition of aqueous ciprofloxacin: transformation products and residual antibacterial activity, Water Res. 44 (10) (2010) 3121–3132.

[14] S. Li, J. Hu, Transformation products formation of ciprofloxacin in UVA/LED and UVA/LED/TiO_2 systems: Impact of natural organic matter characteristics, Water Res. 132 (2018) 320–330.

[15] J.F. Gomes, I. Leal, K. Bednarczyk, M. Gmurek, M. Stelmachowski, A. Zaleska-Medynska, M.E. Quinta-Ferreira, R. Costa, R.M. Quinta-Ferreira, R.C. Martins, Detoxification of parabens using UV-A enhanced by noble metals—TiO_2 supported catalysts, J. Environ. Chem. Eng. 5 (4) (2017) 3065–3074.

[16] T. Suwannaruang, J.P. Hildebrand, D.H. Taffa, M. Wark, K. Kamonsuangkasem, P. Chirawatkul, K. Wantala, Visible light-induced degradation of antibiotic ciprofloxacin over Fe–N–TiO_2 mesoporous photocatalyst with anatase/rutile/brookite nanocrystal mixture, J. Photochem. Photobiol. A: Chem. 391 (2020) 112371.

[17] S. Karuppaiah, A. Raja, M. Arunpandian, K. Stalindurai, P. Rajasekaran, P. Sami, E. R. Nagarajan, M. Swaminathan, Efficient photocatalytic degradation of ciprofloxacin and bisphenol A under visible light using Gd2WO6 loaded ZnO/bentonite nanocomposite, Appl. Surf. Sci. 481 (2019) 1109–1119.

[18] T. Paul, P.L. Miller, T.J. Strathmann, Visible-light-mediated TiO_2 photocatalysis of fluoroquinolone antibacterial agents, Environ. Sci. Technol. 41 (13) (2007) 4720–4727.

[19] R.W. Matthews, Photo-oxidation of organic material in aquaous suspensions of titanium dioxide, Water Res. 20 (5) (1986) 569–578.

[20] R. Dewil, D. Mantzavinos, I. Poulios, M.A. Rodrigo, New perspectives for advanced oxidation processes, J. Environ. Manage. 195 (2017) 93–99.

[21] S. Bettini, E. Boutet-Robinet, C. Cartier, C. Coméra, E. Gaultier, J. Dupuy, N. Naud, S. Taché, P. Grysan, S. Reguer, N. Thieriet, M. Réfrégiers, D. Thiaudière, J.-P. Cravedi, M. Carrière, J.-N. Audinot, F.H. Pierre, L. Guzylack-Piriou, E. Houdeau, Food-grade TiO_2 impairs intestinal and systemic immune homeostasis, initiates preneoplastic lesions and promotes aberrant crypt development in the rat colon, Sci. Rep. (2017) 40373, 20 January.

[22] R. Ahmad, Z. Ahmad, A.U. Khan, N.R. Mastoi, M. Aslam, J. Kim, Photocatalytic systems as an advanced environmental remediation: recent developments, limitations and new avenues for applications, J. Environ. Chem. Eng. 4 (2016) 4143–4164.

[23] P. Dulian, W. Nachit, J. Jaglarz, P. Zieba, J. Kanak, W. Zukowski, Photocatalytic methylene blue degradation on multilayer transparent TiO_2 coatings, Opt. Mater. 90 (2019) 264–272.

[24] D. Schiemann, P. Alphonse, P.-L. Taberna, Synthesis of high surface area TiO_2 coatings on stainless steel by electrophoretic deposition, J. Mater. Res. 28 (15) (2013) 2023–2030.

[25] C. Andriantsiferana, E.F. Mohamed, H. Delmas, Photocatalytic degradation of an azo-dye on TiO_2/activated carbon composite material, Environ. Technol. (2013) 1–9.

[26] M.G. Alalm, A. Tawfik, S. Ookawara, Enhancement of photocatalytic activity of TiO_2 by immobilization on activated carbon for degradation of pharmaceuticals, J. Environ. Chem. Eng. 4 (2016) 1929–1937.

[27] L. Suhadolnik, A. Pohar, U. Novak, B. Likozar, A. Mihelič, M. Čeh, Continuous photocatalytic, electrocatalytic and photo-electrocatalytic degradation of a reactive textile dye for wastewater-treatment processes: batch, microreactor and scaled-up operation, J. Ind. Eng. Chem. 72 (2019) 178–188.

[28] H.K. Hakki, S. Allahyari, N. Rahemi, M. Tasbihi, The role of thermal annealing in controlling morphology, crystal structure and adherence of dip coated TiO_2 film on glass and its photocatalytic activity, Mater. Sci. Semicond. Process. 85 (2018) 24–32.

[29] R.T. Bento, O.V. Correa, M.F. Pillis, Photocatalytic activity of undoped and sulfur-doped TiO_2 films grown by MOCVD for water treatment under visible light, J. Eur. Ceram. Soc. 39 (2019) 3498–3504.

[30] R. Jiang, W. Wen, Y. Luo, J.-M. Wu, Low temperature synthesis of few-layer titanate nanobelts on Ti mesh and the hot-water induced transformations to highly photocatalytic active titania nanorods, J. Environ. Chem. Eng. 5 (5) (2017) 4676–4683.

[31] J. Carvalho Cardoso, N. Lucchiari, M. Valnice Boldrin Zanoni, Bubble annular photoeletrocatalytic reactor with TiO_2 nanotubes arrays applied in the textile wastewater, J. Environ. Chem. Eng. 3 (2) (2015) 1177–1184.

[32] M. Thukkaram, P. Cools, A. Nikiforov, P. Rigole, T. Coenye, P. Van Der Voort, G. Du Laing, C. Vercruysse, H. Declercq, R. Morent, L. De Wilde, P. De Baets, K. Verbeken, N. De Geyter, Antibacterial activity of a porous silver doped TiO_2 coating on titanium substrates synthesized by plasma electrolytic oxidation, Appl. Surf. Sci. 500 (2020) 144235.

[33] J. Margot, C. Kienle, A. Magnet, M. Weil, L. Rossi, L.F. de Alencastro, C. Abegglen, D. Thonney, N. Chèvre, M. Schärer, D. Barry, Treatment of micropollutants in municipal wastewater: ozone or powdered activated carbon? Sci. Total Environ. 461 (2013) 480–498.

[34] S. Al-Maadheed, I. Goktepe, A.B.A. Latiff, B. Shomar, Antibiotics in hospital effluent and domestic wastewater treatment plants in Doha, Qatar, J. Water Process. Eng. 28 (2019) 60–68.

[35] M. Ateia, M. Gar Alalm, D. Awfa, M.S. Johnson, C. Yoshimura, Modeling the degradation and disinfection of water pollutants by photocatalysts and composites: a critical review, Sci. Total Environ. 698 (2020) 134197.

[36] L. Rizzo, S. Meric, D. Kassinos, M. Guida, F. Russo, V. Belgiorno, Water Res. 43 (2009) 979–988.

[37] N.G. Asenjo, R. Santamaría, C. Blanco, M. Granda, P. Álvarez, R. Menéndez, Correct use of the Langmuir-Hinshelwood equation for proving the absence of a synergy effect in the photocatalytic degradation of phenol on a suspended mixture of titania and activated carbon, Carbon 55 (2013) 62–69.

[38] L. Suhadolnik, A. Pohar, B. Likozar, M. Čeh, Mechanism and kinetics of phenol photocatalytic, electrocatalytic and photoelectrocatalytic degradation in a TiO_2-nanotube fixed-bed microreactor, Chem. Eng. J. 303 (2016) 292–301.

[39] K. González-Labrada, R. Richard, C. Andriantsiferana, H. Valdés, U.J. Jáuregui-Haza, M.-H. Manero, Enhancement of ciprofloxacin degradation in aqueous system by heterogeneous catalytic ozonation, Environ. Sci. Pollut. Res. - Int. (2018).

[40] A.I. Caço, F. Varanda, M.J. Pratas de Melo, A.M.A. Dias, R. Dohrn, I.M. Marrucho, Solubility of Antibiotics in Different Solvents. Part II. Non-Hydrochloride Forms of Tetracycline and Ciprofloxacin, Ind. Eng. Chem. Res. 47 (2008) 8083–8089.

[41] C. Sarantopoulos, Photocatalyseurs à Base De TiO2 Préparés Par Infiltration Chimique En Phase Vapeur (CVI) Sur Supports Microfibreux, 19, 2007, 10 [Online]. Available: [Accessed 13 02 2020], http://ethesis.inp-toulouse.fr/archive/00000545/.

[42] M. Al-Mamun, S. Kader, M. Islam, M. Khan, Photocatalytic activity improvement and application of UV-$TiO2$ photocatalysis in textile wastewater treatment, J. Environ. Chem. Eng. 7 (103248) (2019).

[43] B.D. Viezbicke, S. Patel, B.E. Davis, D.P. Birnie, Evaluation of the Tauc method for optical absorption edge determination ZnO thin films as a model system, Phys. Status Solidi B 252 (8) (2015) 1700–1710.

[44] A. Miquelot, O. Debieu, V. Rouessac, C. Villeneuve, N. Prud'homme, J. Cure, V. Constantoudis, G. Papavieros, S. Roualdes, C. Vahlas, TiO_2 nanotree films for the production of green $H_2$by solar water splitting: From microstructural and optical characteristics to the photocatalytic properties, Appl. Surf. Sci. 494 (2019) 1127–1137.

[45] X. Van Doorslaer, K. Demeestere, P.M. Heynderickx, H. Van Langenhove, J. Dewulf, UV-A and UV-C induced photolytic and photocatalytic degradation of aqueousciprofloxacin and moxifloxacin: reaction kinetics and role of adsorption, Appl. Catal. B: Environ. 101 (2011) 540–547.

[46] A. Salma, S. Thoröe-Boveleth, T.C. Schmidt, J. Tuerk, Dependence of transformation product formation on pH duringphotolytic and photocatalytic degradation of ciprofloxacin, J. Hazard. Mater. 313 (2016) 49–59.

[47] S. Murgolo, S. Franz, H. Arab, M. Bestetti, E. Falletta, G. Mascolo, Degradation of emerging organic pollutants in wastewater effluents by electrochemical photocatalysis on nanostructured TiO_2 meshes, Water Res. 164 (2019).

[48] L. Cox, M. Hermosin, J. Cornejo, M. Mansour, Photolysis of metamitron in water in the presence of soils and soil components, Chemosphere 33 (10) (1996) 2057–2064.

[49] Z. Zhang, X. Xie, Z. Yu, H. Cheng, Influence of chemical speciation on photochemical transformation of three fluoroquinolones (FQs) in water: kinetics, mechanism, and toxicity of photolysis products, Water Res. 148 (2019) 19–29.

[50] Y. Schälte, P. Stapor, J. Hasenauera, Evaluation of derivative-free optimizers for parameter estimation in systems biology, IFAC PapersOnLine 51 (19) (2018) 98–101.

[51] S. Kirkpatrick, C.D. Gelatt, M.P. Vecchi, Optimization by simulated annealing, Science 220 (1983) 671–680.

[52] M.J. Arlos, R. Liang, L.C. Li Chun Fong, N.Y. Zhou, C.J. Ptacek, S.A. Andrews, M. R. Servos, Influence of methanol when used as a water-miscible carrier of pharmaceuticals in TiO_2 photocatalytic degradation experiments, J. Environ. Chem. Eng. 5 (2017) 4497–4505.

[53] J.G. Speight, Redox transformations. Reaction Mechanisms in Environmental Engineering, 2018.
[54] X. Gao, Q. Guo, G. Tang, W. Peng, Y. Luo, D. He, Effects of inorganic ions on the photocatalytic degradation of carbamazepine, J. Water Reuse Desalin. 09.3 (2019) 301–309.
[55] G. Zhang, X. He, M.N. Nadagouda, K.E. O'Shea, D.D. Dionysiou, The effect of basic pH and carbonate ion on the mechanism of photocatalytic destruction of cylindrospermopsin, Water Res. 73 (2015) 353–361.